

Have you been using the wrong estimator? These guys bound average fidelity using this one weird trick von Neumann didn't want you to know

Christopher Ferrie^{1,2} and Richard Kueng^{3,2}

¹ Center for Quantum Information and Control, University of New Mexico, Albuquerque, New Mexico, 87131-0001

²Centre for Engineered Quantum Systems, School of Physics, The University of Sydney, Sydney, NSW, Australia

³Institute for Physics, University of Freiburg, Rheinstrasse 10, 79104 Freiburg, Germany

(Dated: July 2, 2022)

We give bounds on the average fidelity achievable by any quantum state estimator, which is arguably the most prominently used figure of merit in quantum state tomography. Moreover, these bounds can be computed online—that is, while the experiment is running. We show numerically that these bounds are quite tight for relevant distributions of density matrices. We also show that the Bayesian mean estimator is ideal in the sense of performing close to the bound without requiring optimization. Our results hold for all finite dimensional quantum systems.

Inferring a quantum mechanical description of a physical system is equivalent to assigning it a quantum state—a process referred to as *tomography*. Tomography is now a routine task for designing, testing and tuning qubits in the quest of building quantum information processing devices [1]. In determining how “good” one is performing this task, a figure of merit must be reported. By far the most commonly used figure of merit for quantum states is *fidelity* [2, 3]. Nowadays, fidelity is used to compare quantum states and processes in a wide variety of tasks, from quantum chaos to quantum control to the continuous monitoring of quantum systems [4–10]. It is surprising then, that the technique which optimizes performance with respect to fidelity is not known.

In [Theorem 3](#), we provide an absolute benchmark for average fidelity performance of any tomographic estimation strategy. This is important because, in the field of quantum tomography, a common theme is to compare estimators. Up to date, many options are available: linear inversion [1], maximum likelihood [11], Bayesian mean [12], hedged maximum likelihood [13], and compressed sensing [14]—to name a few. Often estimators are compared by simulating measurements on ensembles of states drawn according to some measure and averaging the fidelity. This can only provide conclusions about the relative performance of estimators. Thus, our bounds can be used to benchmark the fidelity performance of other candidate estimators.

We complement our theoretical findings with numerical experiments. These demonstrate the relative tightness of our bounds and, in particular, reveal that the Bayesian mean estimator is an excellent choice—owing to its near-optimal performance and ease of implementation. Importantly, both the mean of the distribution and our bounds can be computed *online*—that is, the estimator and its performance can be computed while data is being taken. In the context of Bayesian quantum information theory [12], our findings lend credence to the standard approach of using the mean of the posterior distribution as an estimator is a near-optimal one.

We note that this problem has been solved for the case

of a single qubit ($d = 2$). Bagan *et al* [6] have given the optimal estimator (and measurement!) for any isotropic prior measure. Unfortunately, by making heavy use of the Bloch representation of a qubit, the methods do not generalize. Whereas, our bound holds for all distributions of states in any dimension and coincides with the results of [6] for the case of a single qubit.

The problem of tomography.—Let \mathcal{H} be a Hilbert space of dimension d . Denote state space by

$$\mathcal{S} := \{\sigma \in L(\mathcal{H}) : \sigma \geq 0, \text{Tr}(\sigma) = 1\} \quad (1)$$

The *fidelity* between two states $\rho, \sigma \in \mathcal{S}$ is defined to be [2, 3]

$$F(\rho, \sigma) := \|\sqrt{\rho}\sqrt{\sigma}\|_1^2 = \left[\text{Tr} \sqrt{\sqrt{\rho}\sigma\sqrt{\rho}} \right]^2. \quad (2)$$

Define the average fidelity with respect to some measure $d\rho$ as $\mathbb{E}_\rho[F(\rho, \sigma)]$ [31]. We want the average of this to be as large as possible. Thus, the problem can be succinctly stated as follows:

$$\begin{aligned} &\text{maximize} && \mathbb{E}_\rho[F(\rho, \sigma)] \\ &\text{subject to} && \text{Tr}(\sigma) = 1, \\ & && \sigma \geq 0. \end{aligned} \quad (3)$$

In the context of tomography, we think of ρ as the “true state” and σ as the estimated state. An *estimator* is a function from the space of data to quantum states $\sigma : \text{data} \mapsto \sigma(\text{data}) \in \mathcal{S}$, where data are the results of a sequence of quantum measurements. Since both the true state and data are unknown, we take the expected value with respect to the joint distribution of (ρ, data) to obtain the average fidelity:

$$f(\sigma) = \mathbb{E}_{\rho, \text{data}}[F(\rho, \sigma(\text{data}))]. \quad (4)$$

We want this to be as large as possible. The estimator which maximizes this quantity is equivalent to the estimator maximizing the following posterior average fidelity for every data set:

$$f(\sigma|\text{data}) = \mathbb{E}_{\rho|\text{data}}[F(\rho, \sigma(\text{data}))]. \quad (5)$$

An estimator which maximizes this is called a *Bayes estimator* [32]. Bayes estimators are useful both to understand Bayesian optimality and to provide upper bounds for the worst case performance.

Now here is the subtle and important point. The measurements performed, the data themselves and the distribution from which they were generated are not important once the posterior distribution has been calculated. If we know the solution for every measure $d\rho$, then we know the solution for the posterior measure $d\rho|_{\text{data}}$. For brevity, then, we will drop this conditional information from now on and the problem reduces again to (3).

Ensembles of pure states.—We first present the analytically soluble case of measures supported only on pure states. Such a case is common in theoretical studies which average the performance of their protocols over the popular choice of the unique Haar invariant measure on pure states. The solution is organized into the following theorem:

Theorem 1. *Let the dimension d be arbitrary and assume that the integration measure $d\rho$ is supported only on pure states. Then, the state which solves the optimization problem (3) is the eigenvector of $\mathbb{E}_\rho[\rho]$ with maximal eigenvalue. It achieves a maximal fidelity of $\|\mathbb{E}_\rho[\rho]\|_\infty$.*

The proof is a simple exercise in linear programming. When ρ is a pure state, the fidelity simplifies to $F(\rho, \sigma) = \text{Tr}(\rho\sigma)$. Linearity allows us to bring the expectation inside the trace so that the problem becomes

$$\begin{aligned} & \text{maximize} && \text{Tr}(\mathbb{E}_\rho[\rho]\sigma) \\ & \text{subject to} && \text{Tr}(\sigma) = 1, \\ & && \sigma \geq 0. \end{aligned} \quad (6)$$

The solution can be found in many textbooks covering linear programming—e.g. [17]. This solution also coincides with the one noted for a distribution supported on two states in [18].

General measures on mixed states.—For measures with support on mixed states, the situation is markedly different. Our main technical contribution are new upper bounds for this case. We obtain them by optimizing not the fidelity, but the so-called *super-fidelity*, which provides the following upper bound on the fidelity [19]:

$$F(\rho, \sigma) \leq \text{Tr}(\rho\sigma) + \sqrt{1 - \text{Tr}(\rho^2)}\sqrt{1 - \text{Tr}(\sigma^2)}. \quad (7)$$

For brevity, we define $\hat{\rho} := \mathbb{E}_\rho[\rho]$, $p_\rho := \mathbb{E}_\rho[\sqrt{1 - \text{Tr}(\rho^2)}]$ and the function

$$g(\sigma) := \text{Tr}(\hat{\rho}\sigma) + p_\rho\sqrt{1 - \text{Tr}(\sigma^2)}, \quad (8)$$

such that $\max_{\sigma \in \mathcal{S}} \mathbb{E}_\rho[F(\rho, \sigma)] \leq \max_{\sigma \in \mathcal{S}} g(\sigma)$ holds. The following Lemma allows us to further simplify the maximization of $g(\sigma)$.

Lemma 1. *Fix a density operator ρ with eigenvalue decomposition $\rho = \sum_{i=1}^d r_i |b_i\rangle\langle b_i|$, where the eigenvalues are arranged in non-increasing order (i.e. $r_i \geq r_{i+1}$) and let $\sigma \in \mathcal{S}$ be arbitrary. Then there exists a corresponding density operator $\hat{\sigma}$ with equal purity—i.e. $\text{Tr}(\hat{\sigma}^2) = \text{Tr}(\sigma^2)$ —that commutes with ρ and obeys*

$$\text{Tr}(\rho\sigma) \leq \text{Tr}(\rho\hat{\sigma}). \quad (9)$$

This density operator is explicitly given by

$$\hat{\sigma} = s_i |b_i\rangle\langle b_i|, \quad (10)$$

where s_1, \dots, s_n denote the eigenvalues of σ arranged in non-increasing order.

Proof. The statement follows from a corollary of the Birkhoff-von Neumann Theorem for doubly stochastic matrices—see e.g. [16, Theorem 8.7.6]. For arbitrary hermitian $d \times d$ matrices this corollary assures

$$\text{Tr}(\rho\sigma) \leq \sum_{i=1}^d r_i s_i, \quad (11)$$

where r_i and s_i denote the eigenvalues of ρ and σ , respectively, arranged in non-increasing order. The expression on the right hand side corresponds to $\text{Tr}(\rho\hat{\sigma})$ with $\hat{\sigma}$ defined in (10). Clearly, this $\hat{\sigma}$ is also a quantum state obeying $\text{Tr}(\hat{\sigma}^2) = \text{Tr}(\sigma^2)$, because the spectra of $\hat{\sigma}$ and σ coincide. \square

Lemma 1 allows us to further constrain the maximization of $g(\sigma)$ to density operators $\hat{\sigma}$ which commute with $\hat{\rho}$. Such a refinement is possible, because the lemma assures that for any state σ there is a corresponding one $\hat{\sigma}$, which commutes with $\hat{\rho}$, has equal purity and attains a larger value of $\text{Tr}(\hat{\rho}\hat{\sigma})$. Inserting the explicit form (10) of $\hat{\sigma}$ and optimizing directly over its eigenvalues establishes our second main result:

Theorem 2. *For any finite dimension d and any distribution $d\rho$ over states, let $\hat{r}_1, \dots, \hat{r}_d$ denote the eigenvalues of the mean $\hat{\rho} = \mathbb{E}_\rho[\rho]$. The fidelity achieved by an estimator $\sigma \in \mathcal{S}$ is upper-bounded by the solution of*

$$\begin{aligned} & \text{maximize} && \sum_{i=1}^d \hat{r}_i s_i + p_\rho \sqrt{1 - \sum_{i=1}^d s_i^2} \\ & \text{subject to} && \sum_{i=1}^d s_i = 1, \\ & && s_i \geq 0 \quad 1 \leq i \leq d, \end{aligned} \quad (12)$$

which is a commutative convex optimization problem.

Note that, if the measure $d\rho$ is supported exclusively on pure states, p_ρ vanishes and (12) reduces to **Theorem 1** and becomes tight.

To further understand the nature of such a bound for mixed states and obtain analytical results, we further

relax (12) by replacing the non-negativity constraints ($s_i \geq 0$) by the weaker demand that the optimization vector $(s_1, \dots, s_d)^T \in \mathbb{R}^d$ is contained in the Euclidean unit ball—i.e. $\sum_{i=1}^d s_i^2 \leq 1$. A straightforward application of the method of Lagrange multipliers yields an optimal vector of $\hat{\sigma}$ ’s eigenvalues which corresponds to the matrix

$$\sigma^\sharp = \frac{1}{d} \mathbb{1} + \sqrt{\frac{d-1}{d(p_\rho^2 + \text{Tr}(\hat{\rho}^2)) - 1}} \left(\hat{\rho} - \frac{1}{d} \mathbb{1} \right). \quad (13)$$

Theorem 3. *For any finite dimension d and any distribution $d\rho$ over states, the fidelity achieved by any estimator $\sigma \in \mathcal{S}$ is bounded from above by*

$$\mathbb{E}_\rho[F(\rho, \sigma)] \leq \frac{1}{d} \left(1 + \sqrt{d-1} \sqrt{d \left(\mathbb{E}_\rho \left[\sqrt{1 - \text{Tr}(\rho^2)} \right]^2 + \text{Tr}(\mathbb{E}_\rho[\rho]^2) \right) - 1} \right). \quad (14)$$

We present a more detailed proof of this statement in the [Appendix](#).

Note that since we relaxed the maximization constraints, σ^\sharp in general fails to be positive-semidefinite and is thus not a valid density operator, though we do not use it as such. In particular, the bound is not tight when $d\rho$ is supported only on pure states—as might be evident from the possibility of non-positive states arising from the $(\hat{\rho} - \frac{1}{d}\mathbb{1})$ term in (13). On the other hand, the distribution is known and thus in the case of a distribution supported only on pure states, one should consult the exact solution in [Theorem 1](#).

Conversely, if σ^\sharp happens to be a state, it also solves the optimization (12) and the analytical bound (14) exactly reproduces the—a priori tighter—one presented in [Theorem 2](#). In all of our numerical experiments, some of which are presented below, this was indeed the case.

It is also worthwhile to point out that super-fidelity—the bound in (7)—and the actual fidelity coincide for one qubit, i.e. for $d = 2$ [19]. Also replacing positive semidefiniteness by bounded purity yields the same feasible set for that particular case. Consequently the bound (14) reproduces one of the main results in [6]:

Corollary 1. *In the single-qubit case (i.e. $d = 2$) the bound (14) exactly reproduces the maximum average fidelity in [6, Equation (2.9)] and σ^\sharp is the optimal estimator.*

A proof of this equivalence is provided in the [Appendix](#). There we also further discuss the geometric nature of the relaxation we employed to arrive at [Theorem 3](#).

The best is the enemy of the good.—Note that fidelity achieved by *any* estimator is a lower bound on the one achieved by the optimal estimator. A particularly convenient and generally well motivated [18] estimator is the mean of the distribution $\hat{\rho} = \mathbb{E}_\rho[\rho]$. We want to show that for distributions of states relevant to tomography,

Here, $\mathbb{1}$ denotes the identity matrix. Evaluating the corresponding optimal value yields the following analytical upper bound:

the mean is very near-optimal. In the context of tomography the mean is furthermore arguably the most convenient estimator, since every other quantity of interest requires its calculation anyway.

Finding an analytical expression for the posterior distribution is a very challenging problem, let alone performing the multidimensional integrals required for the calculation of the expectations above. Thus, we turn to numerics. In particular, we use the Sequential Monte Carlo algorithm, which has been successfully applied to quantum statistical problems in the context of dynamical parameter estimation [20–22] and quantum state estimation [23–25].

Recall the sharp distinction between measures supported on pure states and those with full support. We use the fact that we know the exact optimal estimator in the former case to lend support to the claim that the mean estimator is a good candidate for a computationally simple, yet still near-optimal, alternative to solving the optimization problem in general. In [Figure 1](#), we present the results of numerical simulations on two qubits. Plotted is the average fidelity achieved by the optimal estimator (see [Theorem 1](#)) and the mean estimator $\mathbb{E}_\rho[\rho]$. The average is taken with respect to a distribution that begins as the Haar invariant measure on pure states and is updated through simulated measurement data, where the measurement is the “uniform POVM” consisting of all pure states, distributed uniformly according to the Haar measure. For independent measurements—i.e. local, non-adaptive ones—this measurement is optimal [26, Theorem 3.1]. We see that the mean estimator’s fidelity tracks the optimal fidelity quite well.

In [Figure 2](#), we plot the average fidelity of the mean estimator against our bound (14) for measures supported also on mixed quantum states. Again, we simulate measurement data to get an accurate sense of how

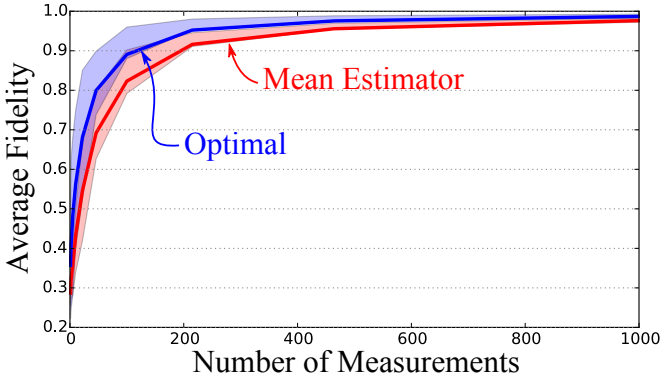


FIG. 1: The average fidelity as a function of the number of single-shot measurements of the Haar uniform measurement. The prior distribution is here is also the Haar uniform measure on two qubits. The lines are the medians and shaded areas the interquartile ranges over 100 trials.

well the average fidelity of the mean estimator performs with respect to our bound for distributions relevant to tomography. In this case, the *prior* distribution is the Hilbert-Schmidt measure [33] and many other natural distributions appear as we update our prior through Bayes' rule. We see again that the mean estimator is a "good" estimator in that it comes close to the bound on the optimal fidelity and is the easiest non-trivial average quantity to evaluate. We have presented some further numerical evidence which favors the Bayesian mean estimator for other mixed state measures in the [Appendix](#).

Conclusion.—In this work we have derived upper bounds on the average fidelity of any estimator with no restrictions on the dimension, or the distribution being averaged over. Furthermore, we have shown a sharp distinction in the optimization problems of maximizing average fidelity between measures supported only on pure states and those with full support. In the former case, we have provided the exact optimal estimator, while in both cases we argued based on numerical evidence that the mean estimator is a good proxy for the optimal solution.

For the curious, we note that the analytical bound (14) (which is based on super-fidelity [19]) is strictly tighter than a corresponding one obtained using the well known, and often used, Fuchs-van de Graaf inequalities [28]. We show this in the [Appendix](#).

These results have obvious applications to practical Bayesian quantum tomography [12], since the bound can be computed *online*—that is, it is only a property of the current distribution under consideration. But we also expect our bound to be of interest in other theoretical work on tomography, where a benchmark is needed to make statements about absolute average performance of some candidate protocol.

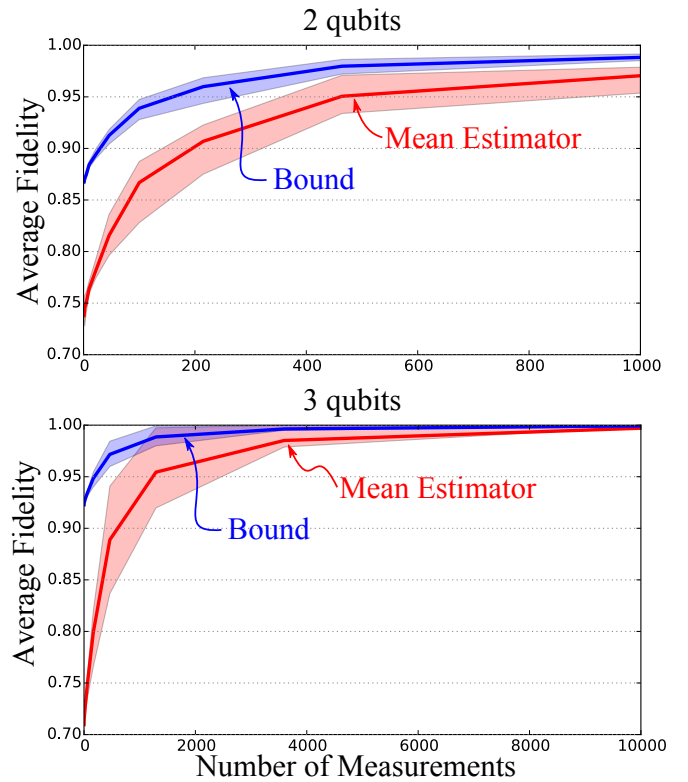


FIG. 2: The average fidelity as a function of the number of single-shot measurements of the Haar uniform measurement. The prior distribution is here is Hilbert-Schmidt measure on two and three qubit mixed quantum states. The lines are the medians and shaded areas the interquartile ranges over 100 trials.

Acknowledgments

We thank Robin Blume-Kohout, Steve Flammia and Patrick Hayden for fruitful discussions. CF was supported by National Science Foundation grant number PHY-1212445, the Canadian Government through the NSERC PDF program, the IARPA MQCO program, the ARC via EQuS project number CE11001013, and by the US Army Research Office grant numbers W911NF-14-1-0098 and W911NF-14-1-0103. RK was supported by scholarship funds from the State Graduate Funding Program of Baden-Württemberg, the Excellence Initiative of the German Federal and State Governments (Grant ZUK 43), the ARO under contracts, W911NF-14-1-0098 and W911NF-14-1-0133 (Quantum Characterization, Verification, and Validation), the Freiburg Research Innovation Fund, and the DFG (GRO 4334-1-1). Furthermore, the authors would like to thank the *Mathematisches Forschungsinstitut Oberwolfach* and the organizers of the Oberwolfach workshop *New Horizons in Statistical Decision Theory* (September 2014, Workshop ID: 1437) where work on this project commenced.

[1] M. A. Nielsen and I. L. Chuang, *Quantum computation and quantum information*. Cambridge University Press (2010).

[2] W. K. Wootters, *Statistical distance and Hilbert space*, *Physical Review D* **23**, 357 (1981).

[3] R. Jozsa, *Fidelity for mixed quantum states*, *Journal of Modern Optics* **41**, 2315 (1994).

[4] Joseph Emerson, Yaakov S. Weinstein, Seth Lloyd and D. G. Cory, *Fidelity Decay as an Efficient Indicator of Quantum Chaos*, *Physical Review Letters* **89**, 284102 (2002).

[5] Navin Khaneja, Timo Reiss, Cindie Kehlet, Thomas Schulte-Herbruggen and Steffen J. Glaser, *Optimal control of coupled spin dynamics: design of NMR pulse sequences by gradient ascent algorithms*, *Journal of Magnetic Resonance* **172**, 296 (2005).

[6] E. Bagan, M. A. Ballester, R. D. Gill, A. Monras and R. Munoz-Tapia, *Optimal full estimation of qubit mixed states*, *Physical Review A* **73**, 032301 (2006).

[7] J. Emerson, M. P. da Silva, O. Moussa, C. A. Ryan, M. Laforest, J. Baugh, D. G. Cory and R. Laflamme *Symmetrized characterization of noisy quantum processes*, *Science* **317**, 1893 (2007).

[8] Steven T. Flammia and Yi-Kai Liu, *Direct fidelity estimation from few Pauli measurements*, *Physical Review Letters* **106**, 230501 (2011).

[9] Marcus P. da Silva, Olivier Landon-Cardinal and David Poulin, *Practical characterization of quantum devices without tomography*, *Physical Review Letters* **107**, 210404 (2011).

[10] Robert L. Cook, Carlos A. Riofrio and Ivan H. Deutsch, *Single-shot quantum state estimation via a continuous measurement in the strong backaction regime*, *Physical Review A* **90**, 032113 (2014).

[11] Z. Hradil, *Quantum-state estimation*, *Physical Review A* **55**, R1561(R) (1997).

[12] Robin Blume-Kohout, *Optimal, reliable estimation of quantum states*, *New Journal of Physics* **12**, 043034 (2010).

[13] Robin Blume-Kohout, *Hedged Maximum Likelihood Quantum State Estimation*, *Physical Review Letters* **105**, 200504 (2010).

[14] David Gross, Yi-Kai Liu, Steven T. Flammia, Stephen Becker and Jens Eisert, *Quantum State Tomography via Compressed Sensing*, *Physical Review Letters* **105**, 150401 (2010).

[15] J. Berger, *Statistical Decision Theory and Bayesian Analysis*. Springer (1985).

[16] Roger A. Horn and Charles R. Johnson, *Matrix analysis (Second edition)*. Cambridge University Press (2013).

[17] S. Boyd, *Convex Optimization*. Cambridge University Press (2004).

[18] Robin Blume-Kohout and Patrick Hayden, *Accurate quantum state estimation via “Keeping the experimentalist honest”*, [arXiv:quant-ph/0603116](https://arxiv.org/abs/quant-ph/0603116).

[19] J. A. Miszczak, Z. Pucha, P. Horodecki, A. Uhlmann, K. Zyczkowski, *Sub- and super-fidelity as bounds for quantum fidelity*, *Quantum Information & Computation* **9**, 103 (2009).

[20] Bradley A. Chase and J. M. Geremia, *Single-shot parameter estimation via continuous quantum measurement*, *Physical Review A* **79**, 022314 (2009).

[21] Christopher E Granade, Christopher Ferrie, Nathan Wiebe and D G Cory, *Robust online Hamiltonian learning*, *New Journal of Physics* **14**, 103013 (2012).

[22] Nathan Wiebe, Christopher Granade, Christopher Ferrie and D.G. Cory, *Hamiltonian Learning and Certification Using Quantum Resources*, *Physical Review Letters* **112**, 190501 (2014).

[23] F. Huszar and N. M. T. Housby, *Adaptive Bayesian quantum tomography*, *Physical Review A* **85**, 052120 (2012).

[24] Christopher Ferrie, *High posterior density ellipsoids of quantum states*, *New Journal of Physics* **16**, 023006 (2014).

[25] Christopher Ferrie, *Quantum model averaging*, *New Journal of Physics* **16**, 093035 (2014).

[26] A. S. Holevo, *Probabilistic and Statistical Aspects of Quantum Theory*. North-Holland Publishing Company (1982).

[27] Karol Zyczkowski, Karol A. Penson, Ion Nechita and Benoit Collins, *Generating random density matrices*, *Journal of Mathematical Physics* **52**, 062201 (2011).

[28] Christopher A Fuchs and Jeroen Van De Graaf, *Cryptographic distinguishability measures for quantum-mechanical states*, *IEEE Transactions on Information Theory* **45**, 1216 (1999).

[29] Martin Henk, *Löwner-John ellipsoids*, *Documenta Mathematica, Extra Volume: Optimization Stories*, 95 (2012).

[30] Christopher Granade and Christopher Ferrie, *QInfer: Library for Statistical Inference in Quantum Information*, (2012).

[31] Expectation values will always be denote with a subscript which specifies the implicit distribution of variables being averaged over.

[32] The terminology and objective functions used here can be seen as standard generalizations of those familiar in decision theory. See, e.g., [15].

[33] See [27] for an overview of canonical ensembles of density matrices and recipes for their construction.

Appendix

Here, we provide detailed proofs of the theoretical results presented in the main text and provide some further insights in the mathematical structure of the tasks at hand. It is organized as follows: In [Section A](#) we provide a more detailed derivation of [Theorem 3](#) by means of Lagrangian multipliers. For the sake of being self-contained and clarifying notational differences, we show how to deduce [6, Equation (2.9)] from the upper bound (14)—[Corollary 1](#) in [Section B](#). In [Section C](#), we employ the Fuchs-van de Graaf inequalities to obtain an alternative upper bound on the total average fidelity. We subsequently show that such a bound is either trivial—i.e. it amounts to one—or strictly majorizes the bound presented in [Theorem 3](#). [Section D](#) further discusses the geometric properties of the convex relaxation we have employed to arrive at [Theorem 3](#)—namely replacing positive-semidefiniteness ($s_i \geq 0$) by bounded Euclidean norm ($\sum_{i=1}^d s_i^2$). Finally, in [Section E](#), we outline the methodology of the numerical experiments and provide some supplementary results for other distributions.

A. Detailed proof of Theorem 3

Let $\hat{r}_1, \dots, \hat{r}_d$ denote the eigenvectors of $\hat{\rho} = \mathbb{E}_\rho [\rho]$. From now on we shall represent them as a vector $\hat{\mathbf{r}} = (\hat{r}_1, \dots, \hat{r}_d)^T \in \mathbb{R}^d$. Likewise we shall encompass the scalar optimization variables s_i in the vector $\mathbf{s} \in \mathbb{R}^d$. Furthermore, let $\mathbf{0} = (0, \dots, 0)^T$ and $\mathbf{1} = (1, \dots, 1)^T$ denote the “all-zeros” and “all-ones” vectors on \mathbb{R}^d , respectively. For $\mathbf{x}, \mathbf{y} \in \mathbb{R}^d$, we will also make use of the standard inner product $\langle \mathbf{x}, \mathbf{y} \rangle = \sum_{i=1}^d x_i y_i$ and the vectorial inequality $\mathbf{x} \geq \mathbf{y}$ shall indicate component-wise inequality, i.e. $x_i \geq y_i$ for all $1 \leq i \leq d$.

For arriving at Theorem 3, we need to solve the optimization problem

$$\begin{aligned} \text{maximize } & f(\mathbf{s}) = \langle \hat{\mathbf{r}}, \mathbf{s} \rangle + p_\rho \sqrt{1 - \langle \mathbf{s}, \mathbf{s} \rangle}, \\ \text{subject to } & g(\mathbf{s}) = \langle \mathbf{1}, \mathbf{s} \rangle = 0, \\ & \langle \mathbf{s}, \mathbf{s} \rangle \leq 1. \end{aligned} \quad (15)$$

analytically. We can furthermore assume that $p_\rho > 0$ holds, since otherwise the problem at hand reduces to Theorem 1.

Note that (15) is a convex optimization problem, as it requires maximizing a concave function over a convex set. As such, it has a unique maximum. One way of finding this maximum is to apply standard techniques such as the Karush-Kuhn-Tucker (KKT) multiplier method [17] which are designed to take into account the inequality constraint (16).

However, here we opt for a less direct, but considerably more convenient and less cumbersome approach: We ignore the inequality constraint in (15) for now and employ the standard technique of Lagrangian multipliers (for equality constraints) in order to find the unique critical point \mathbf{s}^\sharp of the optimization. In a second step, we are going to verify that this vector strictly obeys the additional inequality constraint, we have ignored so far, i.e. $\langle \mathbf{s}^\sharp, \mathbf{s}^\sharp \rangle < 1$. This in turn implies that said inequality constraint is not active at the critical point which in retrospect confirms that we were in fact right to ignore the constraint in the first place. Finally, the fact that we face a convex optimization problem assures that this unique critical point indeed yields the sought for global maximum of (15).

In order to find the critical point \mathbf{s}^\sharp in question we define the Lagrangian function

$$L(\mathbf{s}) = f(\mathbf{s}) + \lambda g(\mathbf{s}), \quad (16)$$

where we have—as already announced—ignored the inequality constraint (16). As a consequence, $\lambda \in \mathbb{R}$ denotes the single Lagrangian multiplier associated with the remaining normalization constraint. The necessary condition for an optimal solution of (15) then reads

$$\hat{\mathbf{r}} - \frac{p_\rho \mathbf{s}}{\sqrt{1 - \langle \mathbf{s}, \mathbf{s} \rangle}} + \lambda \mathbf{1} = \mathbf{0}. \quad (17)$$

Taking the inner product of this vector-identity with the “all-ones” vector $\mathbf{1}$ results in

$$0 = \langle \mathbf{1}, \mathbf{0} \rangle = \langle \mathbf{1}, \hat{\mathbf{r}} \rangle - \frac{p_\rho \langle \mathbf{1}, \mathbf{s} \rangle}{\sqrt{1 - \langle \mathbf{s}, \mathbf{s} \rangle}} + \lambda \langle \mathbf{1}, \mathbf{1} \rangle \quad (18)$$

$$= 1 - \frac{p_\rho}{\sqrt{1 - \langle \mathbf{s}, \mathbf{s} \rangle}} + d\lambda, \quad (19)$$

where we have used $\langle \mathbf{1}, \hat{\mathbf{r}} \rangle = \sum_{i=1}^n \hat{r}_i = \text{Tr}(\hat{\rho}) = 1$ and the normalization constraint, which likewise assures $\langle \mathbf{1}, \mathbf{s} \rangle = 1$. This equation allows us to replace $\sqrt{1 - \langle \mathbf{s}, \mathbf{s} \rangle}$ by $\frac{p_\rho}{1+d\lambda}$ and reinserting this into (17) results in the equivalent vector equation

$$\hat{\mathbf{r}} - (1 + d\lambda) \mathbf{s} + \lambda \mathbf{1} = \mathbf{0}. \quad (20)$$

This can be readily inverted to yield

$$\mathbf{s} = \frac{1}{1 + d\lambda} (\hat{\mathbf{r}} + \lambda \mathbf{1}). \quad (21)$$

In order to determine the value of λ , we revisit (19) which demands

$$p_\rho^2 = (1 + d\lambda)^2 (1 - \langle \mathbf{s}, \mathbf{s} \rangle), \quad (22)$$

$$= (1 + d\lambda)^2 - \langle \hat{\mathbf{r}}, \hat{\mathbf{r}} \rangle - 2\lambda \langle \mathbf{1}, \hat{\mathbf{r}} \rangle - \lambda^2 \langle \mathbf{1}, \mathbf{1} \rangle, \quad (23)$$

$$= d(d-1)\lambda^2 + 2(d-1)\lambda + 1 - \text{Tr}(\hat{\rho}^2), \quad (24)$$

where we have once more used $\langle \mathbf{1}, \hat{\mathbf{r}} \rangle = 1$ as well as $\langle \hat{\mathbf{r}}, \hat{\mathbf{r}} \rangle = \sum_{i=1}^n \hat{r}_i^2 = \text{Tr}(\hat{\rho}^2)$. This results in the quadratic equation

$$\lambda^2 + \frac{2}{d}\lambda - \frac{1}{d(d-1)} (p_\rho^2 + \text{Tr}(\hat{\rho}^2) - 1) \quad (25)$$

for λ whose two possible solutions correspond to

$$\lambda_\pm = -\frac{1}{d} \left(1 \mp \sqrt{\frac{d(p_\rho^2 + \text{Tr}(\hat{\rho}^2)) - 1}{d-1}} \right). \quad (26)$$

Note that the argument of the square-root is non-negative, because the purity $\text{Tr}(\hat{\rho}^2)$ of any quantum state is lower-bounded by $1/d$. Also, the second solution λ_- is vacuous, since it leads to an immediate contradiction. Indeed, it follows by inspection that $\lambda_- < 1/d$ holds. Together with (19) this implies the contradictory relation

$$\sqrt{1 - \langle \mathbf{s}, \mathbf{s} \rangle} = \frac{p_\rho}{1 + d\lambda_-} < 0, \quad (27)$$

because p_ρ is positive by assumption.

Consequently we are left with one meaningful value λ_+ for the Lagrangian multiplier and inserting it into into (21) yields the unique critical solution

$$\mathbf{s}^\sharp = \frac{1}{d} \mathbf{1} + \sqrt{\frac{d-1}{d(p_\rho^2 + \text{Tr}(\hat{\rho}^2)) - 1}} \left(\hat{\mathbf{r}} - \frac{1}{d} \mathbf{1} \right). \quad (28)$$

Recall that throughout this proof we are exploiting a one-to-one correspondence between vectors $s = (s_1, \dots, s_n)^T \in \mathbb{R}^d$ and hermitian $d \times d$ -matrices $\sigma = \sum_{i=1}^n s_i |b_i\rangle\langle b_i|$ that commute with $\hat{\rho}$. Consequently, the critical vector s^\sharp corresponds to the critical matrix presented in (15).

Plugging the critical point s^\sharp into the objective function $f(s)$ furthermore yields the corresponding critical function value

$$f(s^\sharp) = \langle \hat{r}, s^\sharp \rangle + p_\rho \sqrt{1 - \langle s^\sharp, s^\sharp \rangle}, \quad (29)$$

$$= \frac{\langle \hat{r}, \hat{r} \rangle + \lambda_+ \langle \mathbf{1}, \hat{r} \rangle}{1 + d\lambda_+} + \frac{p_\rho^2}{1 + d\lambda_+}, \quad (30)$$

$$= \frac{d(p_\rho^2 + \text{Tr}(\hat{\rho}^2)) - 1 + 1 + d\lambda_+}{d(1 + d\lambda_+)}, \quad (31)$$

$$= \frac{1}{d} \left(1 + \frac{d(p_\rho^2 + \text{Tr}(\hat{\rho}^2)) - 1}{1 + d\lambda_+} \right), \quad (32)$$

$$= \frac{1}{d} \left(1 + \sqrt{d-1} \sqrt{d(p_\rho^2 + \text{Tr}(\hat{\rho}^2)) - 1} \right), \quad (33)$$

where we have once more replaced $\sqrt{1 - \langle s_+^\sharp, s_+^\sharp \rangle}$ by $\frac{p_\rho}{1 + d\lambda_+}$ and combined that with the fact that $(1 + d\lambda_+) = \sqrt{\frac{d(p_\rho^2 + \text{Tr}(\hat{\rho}^2)) - 1}{d-1}}$ holds.

With such a unique critical point s^\sharp at hand, we are now ready to show that it strictly obeys the inequality constraint $\langle s^\sharp, s^\sharp \rangle$ we have ignored so far. By employing the same equalities we have used in the previous paragraph, we can readily establish such a claim:

$$\langle s^\sharp, s^\sharp \rangle = 1 - (1 - \langle s^\sharp, s^\sharp \rangle) = 1 - \frac{p_\rho^2}{(1 + d\lambda_+)^2} < 1. \quad (34)$$

The strict inequality on the right follows from the fact that $p_\rho > 0$ holds by assumption. This indeed establishes, that s^\sharp is also a critical point of the optimization problem (15). Since this optimization corresponds to maximizing a concave function over a convex set, the unique critical point s^\sharp must correspond to the unique maximum of (15). The corresponding objective function value was calculated in (33) and establishes [Theorem 3](#).

B. Proof of [Corollary 1](#)

We start this section by pointing out that in the particular case of dimension $d = 2$, the two relaxations we

have employed in the previous subsection are no relaxations at all. Indeed, for dimension two, fidelity and super-fidelity coincide, as does the standard simplex Δ^1 and its outer approximation $\mathcal{E}_{\Delta^{d-1}}$. Consequently, in this particular low-dimensional case, we solve the actual problem of interest.

For deducing the claimed statement from this fact, we consider Equation (2.9) in [6]:

$$F = \frac{1}{2} \left(1 + \sum_{\chi} \|\mathbf{V}_{\chi}\|_2 \right). \quad (35)$$

Here χ simply means the the data generated via the measurement. The vector \mathbf{V}_{χ} is defined as follows:

$$\mathbf{V}_{\chi} = \mathbb{E}_{\rho}[\mathbf{r} \Pr(\chi|\rho)], \quad (36)$$

where \mathbf{r} is related to the usual Bloch vector $\mathbf{r} = (x, y, z)$ via

$$\mathbf{r} = \left(\sqrt{1 - \|\hat{r}\|_2^2}, \mathbf{r} \right). \quad (37)$$

We point out that this F is not the same average fidelity we have considered but the following quantity (which corresponds to (4)):

$$F = \max_{\sigma} \mathbb{E}_{\rho} \left[\mathbb{E}_{\chi|\rho} [F(\rho, \sigma(\chi))] \right]. \quad (38)$$

Note, however that, by employing Bayes' rule, this is equal to

$$F = \max_{\sigma} \mathbb{E}_{\chi} \left[\mathbb{E}_{\rho|\chi} [F(\rho, \sigma(\chi))] \right], \quad (39)$$

and thus maximizing the posterior average fidelity is equivalent to maximizing the total average fidelity. Our bound applies directly to the former but trivially extends to the latter.

Thus, to prove [Corollary 1](#), we need to extract the posterior average fidelity from the expressions above. First, using Bayes' rule, we calculate

$$\mathbf{V}_{\chi} = \Pr(\chi) \mathbb{E}_{\rho|\chi} [\mathbf{r}]. \quad (40)$$

Using the fact that $\|\mathbf{r}\|_2^2 = 2\text{Tr}(\rho^2) - 1$ and

$$\text{Tr}(\mathbb{E}_{\rho|\chi} [\rho]^2) = \frac{1}{2} \left(1 + \left\| \mathbb{E}_{\rho|\chi} [\mathbf{r}] \right\|_2^2 \right), \quad (41)$$

we find

$$\|\mathbf{V}_\chi\|_2^2 = \Pr(\chi)^2 \left(2\mathbb{E}_{\rho|\chi} \left[\sqrt{1 - \text{Tr}(\rho^2)} \right]^2 + 2\text{Tr}(\mathbb{E}_{\rho|\chi}[\rho]^2) - 1 \right). \quad (42)$$

Plugging this back into (35), we have

$$F = \frac{1}{2} \left(1 + \sum_\chi \Pr(\chi) \sqrt{2\mathbb{E}_{\rho|\chi} \left[\sqrt{1 - \text{Tr}(\rho^2)} \right]^2 + 2\text{Tr}(\mathbb{E}_{\rho|\chi}[\rho]^2) - 1} \right), \quad (43)$$

$$= \frac{1}{2} \left(1 + \mathbb{E}_\chi \left[\sqrt{2\mathbb{E}_{\rho|\chi} \left[\sqrt{1 - \text{Tr}(\rho^2)} \right]^2 + 2\text{Tr}(\mathbb{E}_{\rho|\chi}[\rho]^2) - 1} \right] \right), \quad (44)$$

$$= \mathbb{E}_\chi \left[\frac{1}{2} \left(1 + \sqrt{2\mathbb{E}_{\rho|\chi} \left[\sqrt{1 - \text{Tr}(\rho^2)} \right]^2 + 2\text{Tr}(\mathbb{E}_{\rho|\chi}[\rho]^2) - 1} \right) \right]. \quad (45)$$

Thus, implied by the results of [6], the maximum posterior average fidelity (dropping the χ for parallelism) is

$$\max_\sigma \mathbb{E}_\rho[F(\rho, \sigma)] = \frac{1}{2} \left(1 + \sqrt{2 \left(\mathbb{E}_\rho \left[\sqrt{1 - \text{Tr}(\rho^2)} \right]^2 + \text{Tr}(\mathbb{E}_\rho[\rho]^2) \right) - 1} \right). \quad (46)$$

This however is just our result (14) for dimension $d = 2$.

C. An alternative bound obtained via the Fuchs-van de Graaf inequalities

As already mentioned in the main text's conclusion, a more straightforward approach for obtaining an upper bound on the maximal average fidelity can be obtained by evoking the Fuchs-van de Graaf inequality [28]. These relate the fidelity (2) of two arbitrary quantum states $\rho, \sigma \in \mathcal{S}$ to their total variational distance:

$$1 - \sqrt{F(\rho, \sigma)} \leq \frac{1}{2} \|\rho - \sigma\|_1 \leq \sqrt{1 - F(\rho, \sigma)}.$$

Combining the right hand side of this inequality chain with the standard norm equivalence $\|\rho - \sigma\|_2 \leq \|\rho - \sigma\|_1$ yields the bound

$$F(\rho, \sigma) \leq 1 - \frac{1}{4} \|\rho - \sigma\|_1^2 \leq 1 - \frac{1}{4} \|\rho - \sigma\|_2^2 \quad (47)$$

which holds for any two quantum states $\rho, \sigma \in \mathcal{S}$. Moreover it allows for establishing the following alternative bound relatively straightforwardly:

Theorem 4. *For any finite dimension d and any distribution $d\rho$, the fidelity achieved by any estimator $\sigma \in \mathcal{S}$ obeys*

$$\max_{\sigma \in \mathcal{S}} \mathbb{E}_\rho[F(\rho, \sigma)] \leq 1 - \frac{1}{4} \left(\text{Tr}(\mathbb{E}_\rho[\rho^2]) - \text{Tr}(\mathbb{E}_\rho[\rho]^2) \right). \quad (48)$$

Such a bound is similar to the one presented in Theorem 3, but much easier to establish. However, as the next statement shows, it is strictly weaker than the analytical bound presented in the main text.

Corollary 2. *Let the dimension d and the distribution $d\rho$ over states be arbitrary. Then, the bound (48) obtained via the Fuchs van-de Graaf inequality is either trivial—i.e. equal to one—or it strictly majorizes the one presented in Theorem 3.*

Proof of Theorem 4. Since the relation (58) is valid for any two states ρ, σ it remains true, if we take the expectation over ρ on both sides:

$$\mathbb{E}_\rho[F(\rho, \sigma)] \leq 1 - \frac{1}{4} \mathbb{E}_\rho[\|\rho - \sigma\|_2^2]. \quad (49)$$

Also, we can optimize over σ on both sides to obtain

$$\max_{\sigma \in \mathcal{S}} \mathbb{E}_\rho[F(\rho, \sigma)] \leq 1 - \frac{1}{4} \min_{\sigma \in \mathcal{S}} \mathbb{E}_\rho[\|\rho - \sigma\|_2^2]. \quad (50)$$

The minimum on the right-hand side can in fact be calculated analytically. To this end we define the function

$$h(\sigma) := \mathbb{E}_\rho[\|\rho - \sigma\|_2^2], \quad (51)$$

$$= \text{Tr}(\mathbb{E}_\rho[\rho^2]) - 2\text{Tr}(\mathbb{E}_\rho[\rho]\sigma) + \text{Tr}(\sigma^2). \quad (52)$$

Note that $h(\sigma)$ is convex, because it corresponds to a weighted average of convex norm-functions $\|\sigma - \rho\|_2^2$ and its matrix-valued derivative corresponds to

$$h'(\sigma) = -2\mathbb{E}_\rho[\rho] + 2\sigma. \quad (53)$$

This derivative vanishes if and only if $\sigma^\sharp = \mathbb{E}_\rho[\rho]$ holds and convexity of $g(\sigma)$ implies that this critical state corresponds to the unique minimum. The corresponding

function value amounts to

$$h(\sigma^\sharp) = \text{Tr}(\mathbb{E}_\rho[\rho^2]) - \text{Tr}(\mathbb{E}_\rho[\rho]^2) \quad (54)$$

and reinserting this global minimum into (50) yields the desired statement. \square

Proof of Corollary 2. For notational simplicity, let us introduce the short-hand notation

$$s_\rho := \text{Tr}(\mathbb{E}_\rho[\rho^2]) - \text{Tr}(\mathbb{E}_\rho[\rho]^2), \quad (55)$$

such that the Fuchs-van de Graaf bound (48) simply reads $\max_{\sigma \in \mathcal{S}} \mathbb{E}_\rho[F(\rho, \sigma)] \leq 1 - \frac{s_\rho}{4}$. Note furthermore that $0 \leq s_\rho \leq 1$ holds. As already mentioned, the lower bound follows from invoking Jensen's inequality, while the upper bound is a simple consequence of the fact that the purity of any state is at most one. A vanishing s_ρ would correspond to a trivial Fuchs-van de Graaf bound of one which is the first case instance covered by Corollary 2. Therefore we can from now on safely assume that $s_\rho > 0$ holds. Under this assumption we prove the second claim by starting with the bound presented in Theorem 3 and upper-bounding it via a chain of inequalities which will ultimately lead to the bound presented in Theorem 4. Indeed, pick any dimension d and any distribution $d\rho$ over states. Then Jensen's inequality assures

$$\mathbb{E}_\rho \left[\sqrt{1 - \text{Tr}(\rho^2)} \right]^2 \leq 1 - \mathbb{E}_\rho \left[\text{Tr}(\rho^2) \right] \quad (56)$$

and the right hand side of expression (14) can be upper-bounded by

$$= \frac{1}{d} + \frac{\sqrt{d-1}}{d} \sqrt{d-1 - ds_\rho}, \quad (57)$$

because the square root function is monotonically-increasing on the positive reals. Adding and subtracting s_ρ in the last square root and once more invoking monotonicity allows us to continue via

$$\frac{1}{d} + \frac{\sqrt{d-1}}{d} \sqrt{(d-1)(1-s_\rho) + s_\rho}, \quad (58)$$

$$< \frac{1}{d} + \frac{d-1}{d} \sqrt{1-s_\rho}, \quad (59)$$

where we have used $s_\rho > 0$ in the last line to obtain strict inequality. Since the square root is a concave function, the inequality $\sqrt{1-s_\rho} \leq 1 - \frac{1}{2}s_\rho$ is valid for any $s_\rho \leq 1$ and consequently

$$\frac{1}{d} + \frac{d-1}{d} \sqrt{1-s_\rho} \leq 1 - \frac{d-1}{d} s_\rho \quad (60)$$

is true. Finally, we use the simple fact that $\frac{d-1}{d} \leq \frac{1}{2}$ holds for any $d \geq 2$ to arrive at $1 - \frac{1}{4}s_\rho$ which is just the Fuchs-van de Graaf bound. Since a strict inequality sign connects the expressions in lines (58) and (59) the claimed strict majorization follows. \square

D. Geometric interpretation of the relaxation preceding Theorem 3

In order to arrive at the analytical upper bound (14) we have replaced the feasible set

$$\Delta^{d-1} = \left\{ \mathbf{s} \in \mathbb{R}^d : \langle \mathbf{1}, \mathbf{s} \rangle = 1, \mathbf{s} \geq \mathbf{0} \right\} \quad (61)$$

of the optimization in Theorem 2 by

$$\mathcal{E}_{\Delta^{d-1}} = \left\{ \mathbf{s} \in \mathbb{R}^d : \langle \mathbf{1}, \mathbf{s} \rangle = 1, \langle \mathbf{s}, \mathbf{s} \rangle \leq 1 \right\} \quad (62)$$

which is a convex outer approximation Δ^{d-1} . This follows from the basic fact that $x^2 \leq x$ holds for any $x \in [0, 1]$. Since the vector components s_i of any $\mathbf{s} \in \Delta^{d-1}$ have to obey $s_i \in [0, 1]$, we can readily conclude

$$\langle \mathbf{s}, \mathbf{s} \rangle = \sum_{i=1}^d s_i^2 \leq \sum_{i=1}^d s_i = 1. \quad (63)$$

Note that the converse is true if and only if $d = 1, 2$.

Geometrically, the former set corresponds to the standard simplex in \mathbb{R}^d . In this section we prove that the latter one is in fact the minimum volume covering ellipsoid of the standard simplex which furthermore corresponds to a $(d-1)$ -dimensional Euclidean ball. For dimensions two and three this situation is illustrated in Figure 3.

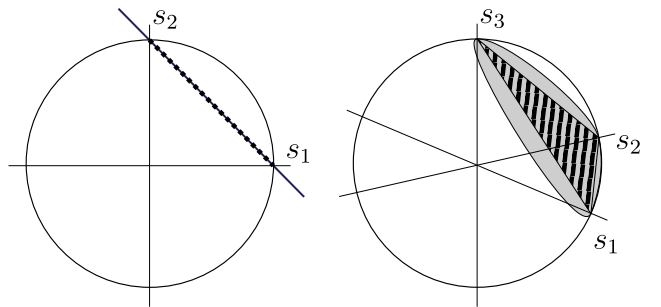


FIG. 3: Geometric relation between the standard simplex Δ^{d-1} and its outer approximation $\mathcal{E}_{\Delta^{d-1}}$: Geometrically, the latter set corresponds to the minimum volume outer ellipsoid of the standard simplex. The figure illustrates this relation for dimensions $d = 2$ and $d = 3$. Note that for $d = 2$, the two sets coincide.

Proposition 1 (Geometric nature of $\mathcal{E}_{\Delta^{d-1}}$). *The convex outer-approximation $\mathcal{E}_{\Delta^{d-1}}$ of the d -simplex corresponds to a $(d-1)$ -dimensional Euclidean ball with radius $\sqrt{\frac{d-1}{d}}$ and center $\frac{1}{\sqrt{d}}\mathbf{1}$ which is contained in the $(d-1)$ -dimensional hyperplane $\mathcal{H}_{1,1} := \left\{ \mathbf{s} \in \mathbb{R}^d : \langle \mathbf{1}, \mathbf{s} \rangle = 1 \right\}$.*

Proof. By definition, the set $\mathcal{E}_{\Delta^{d-1}}$ corresponds to the intersection of the Euclidean unit ball $\mathcal{B}_1(0) = \left\{ \mathbf{s} \in \mathbb{R}^d : \langle \mathbf{s}, \mathbf{s} \rangle \leq 1 \right\}$ and the hyperplane $\mathcal{H}_{1,1}$. This assures $\mathcal{E}_{\Delta^{d-1}} \subseteq \mathcal{H}_{1,1}$ by construction.

One way to establish that $\mathcal{E}_{\Delta^{d-1}}$ is furthermore itself an Euclidean ball, is using “generalized cylindrical coordinates” for the Euclidean unit ball $\mathcal{B}_1(0)$: Such coordinates use the fact that $\mathcal{B}^d(1,0)$ is equivalent to the union of a family of $(d-1)$ -dimensional unit balls. More concretely: let $z \in \mathbb{R}^d$ be an arbitrary unit vector and let $\zeta \in \mathbb{R}$ denote a parameter. For each value of this parameter, we define the hyperplane $\tilde{\mathcal{H}}_{z,\zeta} = \{s \in \mathbb{R}^d : \langle z, s \rangle = \zeta\}$ which in particular contains the vector ζz by construction. Furthermore, let $\tilde{\mathcal{B}}^{d-1}(z, \zeta) \subset \tilde{\mathcal{H}}_{z,\zeta}$ be the $(d-1)$ -dimensional Euclidean ball with radius $\sqrt{1 - \zeta^2}$ and center ζz that is contained in the hyperplane $\tilde{\mathcal{H}}_{z,\zeta}$. Clearly each element in such a union of sets is contained in the d -ball, and letting ζ range from -1 to 1 covers the entire d -ball. In order to see this, decompose any $s \in \mathcal{B}_1^d(0)$ as $s = \langle s, z \rangle z + z^\perp$ such that $\langle z^\perp, z \rangle = 0$ and set $\zeta = \langle s, z \rangle$. Pythagoras’ theorem then assures $\|\zeta^\perp\|_2 \leq \sqrt{1 - \zeta^2}$ and consequently $s \in \tilde{\mathcal{B}}^{d-1}(\zeta, \zeta)$.

The structure of the particular problem at hand suggests to fix $z = \frac{1}{\sqrt{d}}\mathbf{1}$. Indeed, such a particular choice of z assures equality of the hyperplane $\mathcal{H}_{1,1}$ which contains $\mathcal{E}_{\Delta^{d-1}}$ and the hyperplane $\tilde{\mathcal{H}}_{\frac{1}{\sqrt{d}}\mathbf{1}, \frac{1}{\sqrt{d}}}$, we have just introduced. Consequently, the “cylindrical representation” of the Euclidean unit ball assures that the intersection $\mathcal{E}_{\Delta^{d-1}} = \mathcal{B}_1(0) \cap \mathcal{H}_{1,1}$ corresponds to the $(d-1)$ -ball $\tilde{\mathcal{B}}^{d-1}(\frac{1}{\sqrt{d}}\mathbf{1}, \frac{1}{\sqrt{d}})$ associated with the hyperplane $\tilde{\mathcal{H}}_{\frac{1}{\sqrt{d}}\mathbf{1}, \frac{1}{\sqrt{d}}}$ and a parameter value $\zeta = \frac{1}{\sqrt{d}}$. By definition, this ball has center $\frac{1}{d}\mathbf{1}$ and radius $\sqrt{1 - \zeta^2} = \sqrt{\frac{d-1}{d}}$ which completes the proof. \square

The next statement establishes that our choice of replacing the original feasible set Δ^{d-1} in the proof of [Theorem 3](#) by the larger convex set $\mathcal{E}_{\Delta^{d-1}}$ is in a precise sense the tightest possible elliptic relaxation of the original optimization problem.

Proposition 2. *The set $\mathcal{E}_{\Delta^{d-1}}$ is the unique minimal volume covering ellipsoid of the standard simplex Δ^{d-1} .*

The proof exploits the following standard result about Löwner-John ellipsoids that is originally due to John. However, here we make use of a slightly more general version presented in [29].

Theorem 5 (Theorem 2.1 in [29]). *Let $K \subset \mathbb{R}^d$ be a convex body and let K be contained in the Euclidean unit ball $\mathcal{B}^d(0)$. Then the following statements are equivalent:*

1. $\mathcal{B}^d(0)$ is the unique minimum volume ellipsoid containing K .
2. There exist contact points u_1, \dots, u_m lying both in the boundary of K and $\mathcal{B}^d(0)$, and positive numbers

$\lambda_1, \dots, \lambda_m, m \geq d$, such that

$$\sum_{i=1}^m \lambda_i u_i = \mathbf{0} \quad \text{and} \quad \sum_{i=1}^m \lambda_i |u_i\rangle\langle u_i| = \mathbb{1}. \quad (64)$$

Proof. In [Proposition 1](#) we have established that the set $\mathcal{E}_{\Delta^{d-1}}$ corresponds to a $(d-1)$ -ball with radius $\sqrt{\frac{d-1}{d}}$ and center $\frac{1}{d}\mathbf{1}$ that (like the standard simplex) is contained in the hyperplane $\mathcal{H}_{1,1}$. A quick calculation reveals that all vertices of the standard simplex Δ^{d-1} —which are just the standard basis vectors e_1, \dots, e_d —have Euclidean distance $\sqrt{\frac{d-1}{d}}$ to the ball’s center. Consequently they are contained in the boundary of the ball $\mathcal{E}_{\Delta^{d-1}}$ and we have found sufficiently many contact points for applying [Theorem 5](#). Since volume is translationally invariant we can furthermore shift the coordinate’s origin into the point $\frac{1}{d}\mathbf{1}$ (which is the center of the ball $\mathcal{E}_{\Delta^{d-1}}$). This has the advantage that the affine space $\mathcal{H}_{1,1}$ containing both Δ^{d-1} and $\mathcal{E}_{\Delta^{d-1}}$ turns into $\mathcal{H}_{1,0}$ which is a linear subspace. Note that with respect to the (translated) standard basis, the orthogonal projection onto this subspace is given by

$$P = \mathbb{1} - \frac{1}{d}|\mathbf{1}\rangle\langle\mathbf{1}|.$$

With respect to this new coordinate system, the d contact points (vertices of the simplex) amount to $\tilde{e}_i = e_i - \frac{1}{d}\mathbf{1}$. Choosing unit weights $\lambda_i = 1$ for all $m = d$ contact points $u_i = \tilde{e}_i$ and calculating

$$\sum_{i=1}^m \lambda_i u_i = \sum_{i=1}^n \tilde{e}_i = \sum_{i=1}^n \left(e_i - \frac{1}{d}\mathbf{1} \right) = \mathbf{0} \quad (65)$$

reveals that the first condition for [Theorem 5](#) is fulfilled. A similar calculation reveals

$$\sum_{i=1}^m \lambda_i |u_i\rangle\langle u_i| = \mathbb{1} - \frac{1}{d}|\mathbf{1}\rangle\langle\mathbf{1}|.$$

This, however equals just the projector P onto the subspace $\mathcal{H}_{1,0}$ which contains the entire $(d-1)$ -dimensional problem of interest. Restricted to its range, a projector corresponds to the identity which establishes the second condition for [Theorem 5](#). Since this statement is invariant under re-scaling, we can also apply it here, where the radius of the $(d-1)$ -dimensional surrounding Euclidean ball is not one but $\sqrt{\frac{d-1}{d}}$. \square

E. Numerical recipes

As noted in the main text, we use the Sequential Monte Carlo (SMC) algorithm to perform the Bayesian updating and averaging. A complete and detailed discussion of the algorithm appears in Ref. [21] and thus

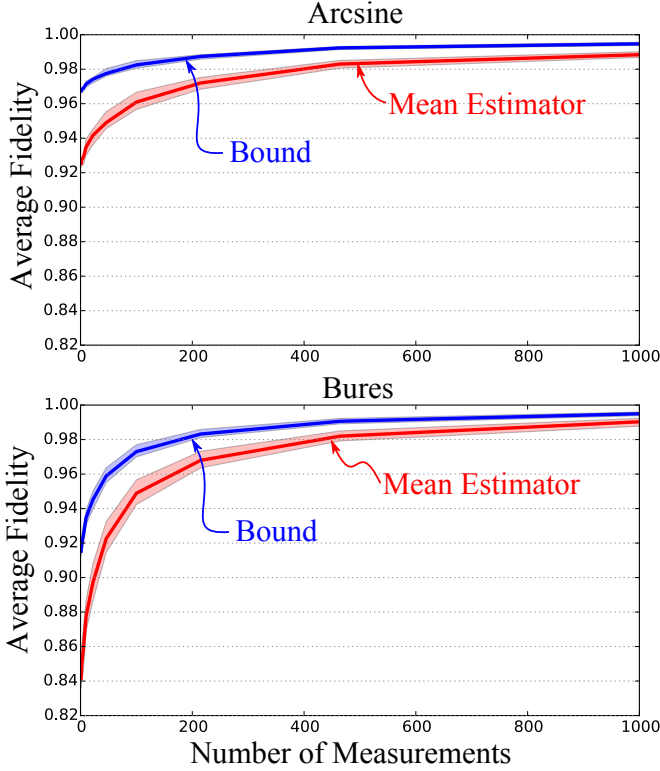


FIG. 4: The average fidelity as a function of the number of single-shot measurements of the Haar uniform measurement. The prior distribution for the upper plot is the *Arcsine* distribution while for the lower plot the *Bures* distribution was used—both are supported on two qubit mixed quantum states (again, see [27] for a review of distributions of density matrices). The lines are the medians and shaded areas the interquartile ranges over 100 trials.

we will not repeat the details here, but we will sketch the

idea. An open-source implementation in Python also exists [30].

The SMC algorithm begins with a set of quantum states $\{\rho_j\}_{j=0}^n$, the elements of which are called *particles*. Here, $n = |\{\rho_j\}|$ is the number of particles and controls the accuracy of the approximation. By approximating the prior distribution by a weighted sum of Dirac delta-functions,

$$\Pr(\rho) \approx \sum_{j=1}^n w_j \delta(\rho - \rho_j), \quad (66)$$

Bayes rule then becomes

$$w_j \mapsto \Pr(\text{data}|\rho_j)w_j, \quad (67)$$

followed by a normalization step. The SMC algorithm is designed to approximate expectation values, such that

$$\mathbb{E}_\rho[f(\rho)] \approx \sum_{j=1}^n w_j f(\rho_j), \quad (68)$$

for any function f . In other words, the SMC algorithm allows us to efficiently compute the multidimensional integrals with respect to the measure defined by the posterior probability distribution. We use this algorithm, as implemented by [30], to compute the expectations appearing in this paper.

In the main text, we considered distributions of density matrices which evolve according to Bayes' rule and begins with the Hilbert-Schmidt prior. Below, in Figure 4 we repeat these experiments with different priors, namely the *arc sine* and *Bures* distributions [27]. We see our conclusion that the mean estimator is “good” remains unchanged.